Effect of phase breaking on ac transport through a quantum dot dimer

T. C. Au Yeung and W. Z. Shangguan
School of Electrical and Electronic Engineering, Nanyang Technological University, Singapore 639798

Q.-H Chen
Department of Physics, Zhejiang University, Hangzhou 310027, China

Y. B. Yu, C. H. Kam, and M. C. Wong
School of Electrical and Electronic Engineering, Nanyang Technological University, Singapore 639798
(Received 25 February 2001; revised manuscript received 6 July 2001; published 13 December 2001)

The ac response of a coupled double quantum dot system involving a phase-breaking effect is studied. We calculate the ac conductance based on the nonequilibrium Green's-function formalism. Some parasitic and gate capacitances are included in our model, thus the displacement current is considered, and the overall charge and current conservation are fulfilled. In our results the double resonant structure of the conductance is observed. We find that the electron-phonon interaction has a significant effect on the ac conductance both for low and high temperatures. Due to the phase-breaking effect of electron-phonon scattering, the resonant conductance peak is suppressed very seriously, and the second peak of the ac conductance may disappear completely, However, for the nonresonant situation, the conductance is enhanced for small frequencies. Furthermore, we study the effect of the capacitances on the ac conductance, and find that, for small frequencies, the capacitances have a small effect on the real part of the admittance. On the imaginary part of the admittance, all the capacitances except for the interdot capacitance have a considerable effect. For high frequencies all the capacitances have a considerable effect on the ac conductance.

DOI: 10.1103/PhysRevB.65.035306 PACS number(s): 73.40.Gk, 73.21.−b

I. INTRODUCTION

ac quantum transport properties of quantum dot systems have attracted much research attention, both experimentally[1–5] and theoretically.[6–17] It has been made clear that under a time-dependent potential the conduction electrons flowing through a mesoscopic semiconductor device, say a quantum dot, will develop an ac sideband weighted by a Bessel function of the amplitude and frequency of the external alternating field. In time-dependent processes, the phase coherent transport of electrons will be affected by the ac-driven forces differently in different parts. In fact, the electrons may absorb external energy to modify their phases, and some nonlinear effects, such as photon-assisted tunneling[8,12] and electron pumps,[17] will exhibit.

Anantram and Datta[7] studied the effect of phase breaking on the ac response of a single quantum dot. However, their results showed that there is hardly any difference in the zero-frequency ac conductance of the one-level resonant-tunneling device between cases with and without electron-phonon interaction, no matter at high or low the temperature. They assumed that in a mesoscopic conductor there is no ac potential. This leads to the supposition that, in such a two-probe system, the left ac current flowing from the left contact into the mesoscopic conductor is not equal to the right current flowing from the conductor into the right contact. Recently, many experimental and theoretical studies were devoted to analyses of the effects of a time-dependent field on the resonant tunneling through coupled double quantum dots.[11–14] While photon-assisted tunneling is intrinsically a coherent phenomenon, the electron-phonon interaction will lead the ac conductance to deviate from the dc value as the frequency of the ac field exceeds the inverse of the time an average electron spends inside the devices.[7] Very recently, Ma *et al.* studied quantum ac transport in coupled quantum dots.[14] They predicted that there are peaks in the average tunneling current which are observable in both the amplitude and phase shift of the ac current. As far as we know, however, there has not yet been a discussion of electron-phonon interaction (or the effect of phase breaking) in ac transport through a tunneling-coupled double-dot system.

In this paper we study the linear ac response of a coupled double quantum dot in the presence of electron-phonon interaction, based on the nonequilibrium Green's-function formalism first proposed by Jauho *et al.* for single-quantum dot systems.[6] We calculate the Keldysh Green's functions for a double dot by the method of the equation of motion (EOM) and contour integration. The EOM was discussed in detail in Ref. 19 while the contour integration was discussed, for example, in Ref. 20. We take the phase-breaking process into account by including the electron-phonon interaction self-energy in the Dyson equations for the nonequilibrium Green's functions. In our model some parasitic capacitances and the internal time-dependent potential in the dots are included, and the internal potential is determined in a self-consistent way. Thus, the displacement current is considered, and the overall charge and current conservations are fulfilled. We also demonstrate the gauge invariance of our result, that is, current and charge responses are invariant under an overall potential shift.

Following the work on a single quantum dot in Ref. 7, we express the general current formula for a coupled double dot in terms of various Keldysh's Green's functions, and then linearize the ac current in the case of a small ac bias. It is

more convenient to use double-energy coordinates in the calculation of various Green's functions and self-energies. Double-energy coordinates are also useful in the description of scattering processes by a time-dependent potential. We numerically compute the ac conductance in various cases of frequency and tunneling coupling. Our results show that the electron-phonon interaction has a significant effect on the ac conductance both for low and high temperatures. In our results a double-resonant structure of the ac conductance is observed at low temperature. Due to the phase-breaking effect, the resonant conductance peak is suppressed very seriously; the second peak of the ac conductance may disappear completely, and nonresonant conductance is enhanced for small frequency. Furthermore, we have studied the effect of parasitic and gate capacitances on ac conductance, and found that for small frequencies the capacitances have a small effect on real part of the admittance. On the other hand, the capacitances, apart from the interdot capacitance, have a considerable effect on the imaginary part. For high frequencies all the capacitances have considerable effects on the ac conductance.

In Sec. II a general formula for the linearized ac current in the double dot is derived. The numerical results for the ac conductance are presented and discussed in Sec. III. Section IV is devoted to our main conclusions.

II. GENERAL FORMALISM

We consider a tunneling-coupled double dot connected to two electron reservoirs by tunnel coupling, which is introduced as a perturbation. Alternating fields are applied to the electron reservoirs in addition to a dc voltage. The system is described by a Hamiltonian

$$H=\sum_{k,\alpha\in L,R}\epsilon_{k\alpha}(t)c_{k\alpha}^{\dagger}c_{k\alpha}+\sum_{i,n}\epsilon_i^0(t)d_{in}^{\dagger}d_{in}+\sum_{n,m}V_{1m2n}(d_{1m}^{\dagger}d_{2n}+\text{H.c.})+\sum_{k,n}[V_{L,n}(c_{kL}^{\dagger}d_{1n}+\text{H.c.})+V_{R,n}(c_{kR}^{\dagger}d_{2n}+\text{H.c.})]+H_{el\text{-}ph}, \quad (1)$$

where $c_{k\alpha}^{\dagger}$ ($c_{k\alpha}$) is the creation (annihilation) operator for electrons in the α reservoir, $d_{in}^{\dagger}$ (d_{in}) is the electron creation (annihilation) operator for the nth level in the ith dot, V_L (V_R) is the tunneling coupling between dot 1 (2) and the left (right) reservoir, and V_{12} is the tunneling coupling between the two dots. The Hamiltonian for the electron-phonon interaction is of the form

$$H_{el\text{-}ph}=\sum_{m,n,\mathbf{q}}M_{m,n,\mathbf{q}}^{(1)}d_{1m}^{\dagger}d_{1n}(b_{1\mathbf{q}}+b_{1\mathbf{q}}^{\dagger})+\sum_{m,n,\mathbf{q}}M_{m,n,\mathbf{q}}^{(2)}d_{2m}^{\dagger}d_{2n}(b_{2\mathbf{q}}+b_{2\mathbf{q}}^{\dagger}), \quad (2)$$

in which $b_{1\mathbf{q}}$ ($b_{2\mathbf{q}}$) annihilates a phonon in dot 1 (2). In writing Eq. (1) we have neglected the time dependence of the tunnel couplings between dots and reservoirs and between the two dots. At a small ac bias this is a valid approximation.[7] We also assume that the tunneling couplings do not depend on the dot levels.

Applying a sinusoidal potential $V_\alpha\cos(\omega_0 t)$ to the α contact causes the electron energies in the contact to vary as $\epsilon_{k\alpha}(t)=\epsilon_{k\alpha}+eV_\alpha\cos(\omega_0 t+\phi_\alpha)$, where $\alpha=1$ and 2. This ac potential results in a time-dependent energy in the two dots: $\epsilon_i^0(t)=\epsilon_i^0+\Delta_i\cos(\omega_0 t+\phi_i)$ ($i=1$ and 2). The ac tunneling current can be calculated based on the Keldysh Green's functions and retarded and lesser self-energies in the two dots,

$$J_{L(R)}^{Tun}(t)=\frac{e}{\hbar}\mathrm{Tr}\int dt_1\{G_{1(2),1(2)}^{r}(t,t_1)\Sigma_{L(R)}^{<}(t_1,t)+G_{1(2),1(2)}^{<}(t,t_1)\Sigma_{L(R)}^{a}(t_1,t)-\Sigma_{L(R)}^{<}(t,t_1)G_{1(2),1(2)}^{a}(t_1,t)-\Sigma_{L(R)}^{r}(t,t_1)G_{1(2),1(2)}^{<}(t_1,t)\}, \quad (3)$$

where

$$G_{im,im}^{<}(t)=i\langle d_{in}^{\dagger}(0)d_{im}(t)\rangle, \quad (4)$$

$$G_{im,in}^{r}(t)=-i\theta(t)\langle\{d_{im}(t),d_{in}^{\dagger}(0)\}\rangle \qquad (i=1,2). \quad (5)$$

The tunneling self-energies are related to the free-particle Green's functions in the electron reservoirs and the tunnel couplings between the contacts and dots:

$$\Sigma_{\alpha,mn}^{r,a,<}(t,t')=V_{\alpha m}^{*}V_{\alpha n}\sum_k g_{k\alpha}^{r,a,<}(t,t') \qquad (\alpha=L,R). \quad (6)$$

Equation (3) is valid in general, even in the presence of strong electron-electron and electron-phonon interactions, and it is applicable to quantum dots with multiple energy levels. As a solvable example, in the following we shall restrict ourselves to the case in which each dot contains only one energy level, i.e., $m=n=1$ in the above equations.

By the method of the equation of motion and Keldysh's contour integration, the retarded and ''lesser'' Green's functions in the two dots can be calculated,[18]

$$G_{ii}^{r}=G_{ii}^{r0}+G_{ii}^{r0}V_{12}G_{\bar{\imath}\bar{\imath}}^{r0}V_{12}G_{ii}^{r}, \quad (7)$$

$$G_{ii}^{<}=G_{ii}^{r}\Sigma_i^{<}G_{ii}^{a}+G_{ii}^{r}V_{12}G_{\bar{\imath}\bar{\imath}}^{r0}\Sigma_{\bar{\imath}}^{<}G_{\bar{\imath}\bar{\imath}}^{a0}V_{12}G_{ii}^{a}, \quad (8)$$

where $i=1$ and 2 and $\bar{i}=3-i$ (we shall use this prescription below in this paper), and G_{ii}^{r0} is defined by

$$G_{ii}^{r0}=g_{ii}^{r0}+g_{ii}^{r0}\Sigma_i^{r}G_{ii}^{r0} \qquad (i=1,2). \quad (9)$$

In the above equation $\Sigma_i^{r,>,<}=\Sigma_\alpha^{r,>,<}+\Sigma_{i\phi}^{r,>,<}$ [$i=1$ (2) corresponds to $\alpha=L(R)$, and we shall follow this prescription below], where Σ_α^{r}, the retarded self-energy due to the tunneling, is given by Eq. (6), while $\Sigma_{i\phi}^{r,>,<}$, the self-energy due to the electron-phonon interaction in the ith dot, is given by

$$\Sigma_{i\phi}^{>,<}(t,t')=-\sum_{\mathbf{q}}(M_{\mathbf{q}}^{(i)})^2D_{i\mathbf{q}}^{>,<}(t,t')G_{ii}^{>,<}(t,t'), \quad (10)$$

$$\Sigma^r_{i\phi}(t,t') = -\sum_{\mathbf{q}} (M^{(i)}_{\mathbf{q}})^2 [G^<_{ii}(t,t') D^r_{i\mathbf{q}}(t,t') + G^r_{ii}(t,t') D^<_{i\mathbf{q}}(t,t') + G^r_{ii}(t,t') D^r_{i\mathbf{q}}(t,t')] \quad (i=1,2), \tag{11}$$

where $D^{r,>,<}_{i\mathbf{q}}(t,t')$ is the phonon Green's function in the dot i and $M^{(i)}_{\mathbf{q}}$ is the phonon coupling. Finally, g^{r0}_{ii} are the free particle Green's functions in the absence of tunneling and electron-phonon interaction. Unlike the case of dc bias where the Green's functions $G^{r,a,<}_{ii}$ have simple expressions in energy representations,[18] in the case of ac bias they are much more complicated but can be calculated in principle by iteration from Eqs. (7) and (8).

In discussing the linear response to a sinusoidal driving signal, it is convenient to transform the double-time coordinates to double-energy coordinates. The Fourier transform from double-time coordinates to double-energy coordinates follows the prescription

$$F(\omega_1,\omega_2) = \int\int dt_1 dt_2 f(t_1,t_2) e^{-i(\hbar\omega_1 t_1 - \hbar\omega_2 t_2)}.$$

For small ac voltages, we can linearize the left (right) current flowing from the left (right) reservoir into dot 1 (2), obtained from Eq. (3) about the steady state, to be

$$\delta J^{Tun}_{\alpha}(\omega) = \frac{e}{\hbar}\int \frac{d\omega_1}{2\pi} \delta\Sigma^<_{\alpha}(-\omega_1-\omega,-\omega_1)[G^r_{ii}(\omega_1+\omega) - G^a_{ii}(\omega_1)] + \delta G^r_{ii}(-\omega_1-\omega,-\omega_1)\Sigma^<_{\alpha}(\omega_1) - \delta G^a_{ii}(-\omega_1-\omega,-\omega_1)\Sigma^<_{\alpha}(\omega_1+\omega) + i\Gamma^{\alpha}\delta G^<_{ii}(\omega_1-\omega,\omega_1) \quad (\alpha = L,R). \tag{12}$$

In Eq. (12) Green's functions and self-energies that have only one energy coordinate are the steady-state functions corresponding to the dc bias. We shall follow this prescription in the following. The steady-state retarded self-energy $\Sigma^r_{\alpha}(\omega)$ is assumed to be of the form $-(i/2)\Gamma^{\alpha}$ [where $\Gamma^{\alpha} = 2\pi\rho(0)|V_{\alpha}|$], this is valid in the wide-band limit. The four terms on the right-hand side of Eq. (12) have different physical meanings. The effect of oscillating an electron reservoir at a frequency ω leads to sidebands $E \pm \hbar\omega$ for each energy E in the contact. The first term here represents the correlated injection into the device due to electrons at energies E and $E \pm \hbar\omega$. The second and third terms represent injections from the contact at one energy to a changing density of states in the device. Finally, the fourth term represents an injection into the contact due to changing charge in the device. We will use the notation δ to denote the first-order change (due to the small ac potential V_{α}) of all important quantities. For example, δG^r_{ii}, $\delta G^<_{ii}$, . . . , and so on. We assume that the phonon Green's function are dispersionless.

To calculate the current response, we expand the Green's functions in the formula of current to first-order term of the external ac voltage V_{α} and internal potential $V_i (= \Delta_i/e)$, and then we have

$$\delta J^{Tun}_{L(R)}(\omega) = \sum_{I=1,2,L,R} G^0_{L(R)I}(\omega) V_I(\omega) - \frac{\Gamma^L}{\hbar} Q_{1(2)}(\omega) \tag{13}$$

and

$$Q_i(\omega) = -ie\int \frac{d\overline{\omega}}{2\pi} \delta G^<_{ii}(\overline{\omega}-\omega,\overline{\omega}) \tag{14}$$

$$= \sum_{I=1,2,L,R} e^2 N_{iI}(\omega) V_I(\omega), \tag{15}$$

where $V_I(\omega) = V_I[\pi\delta(\omega+\omega_0)e^{i\phi_I} + \pi\delta(\omega-\omega_0)e^{-i\phi_I}]$ is the Fourier transform of $V_I(t)$. In Eq. (13), $G^0_{L(R)i}$ are given below:

$$G^0_{L1}(\omega) = \Gamma^L \frac{e^2}{\hbar}\int \frac{d\omega_1}{2\pi}[i f_L(\omega_1) G^r_{11}(\omega_1+\omega) G^r_{11}(\omega_1) + \text{c.c.}(\omega\to-\omega)], \tag{16}$$

$$G^0_{L2}(\omega) = \Gamma^L \frac{e^2}{\hbar} V^2_{12}\int \frac{d\omega_1}{2\pi}[i f_L(\omega_1) G^r_{11}(\omega_1+\omega) G^{r0}_{11}(\omega_1+\omega) G^{r0}_{11}(\omega_1) G^r_{11}(\omega_1) + \text{c.c.}(\omega\to-\omega)], \tag{17}$$

$$G^0_{LL}(\omega) = \Gamma^L \frac{e^2}{\hbar}\int \frac{d\omega_1}{2\pi} \frac{f_L(\omega_1+\omega) - f_L(\omega_1)}{\omega}\{G^r_{11}(\omega_1+\omega) - [G^r_{11}(\omega_1)]^*\}, \tag{18}$$

and

$$G^0_{LR}(\omega) = 0. \tag{19}$$

The symbol c.c.$(\omega\to-\omega)$ in Eqs. (16) and (17) is used for convenience, and it means that we change ω to $-\omega$ in the first term and then take the complex conjugate. Similarly, $G^0_{RI}(\omega)$ can be written.

In the above equations,

$$G^{r0}_{ii}(\omega) = \frac{1}{\omega - \epsilon^0_i + \frac{i}{2}(\Gamma^{\alpha} + \Gamma_{i\phi})}, \tag{20}$$

$$G^r_{11}(\omega) = \frac{1}{\omega_1 - \epsilon^0_1 + \frac{i}{2}(\Gamma^L + \Gamma_{1\phi}) - V^2_{12} G^{r0}_{22}(\omega)}, \tag{21}$$

and

$$G^r_{22}(\omega) = \frac{1}{\omega_1 - \epsilon^0_2 + \frac{i}{2}(\Gamma^R + \Gamma_{2\phi}) - V^2_{12} G^{r0}_{11}(\omega)} \tag{22}$$

are steady-state Green's functions. Also, $Q_{1,2}(\omega)$ are the ac charges in the two dots, and $N_{iJ}(\omega)$ can be obtained by linearizing Eq. (8) and then substituting into Eq. (14). The equations of calculating $N_{iJ}(\omega)$ are given in the Appendix. One more quantity needs to be determined before we can

proceed to obtain $N_{i\,J}(\omega)$. It is the steady state (due to the dc bias) less the self-energy $\Sigma^{<}_{i\phi}(\omega)$. By assuming that the phonon Green's functions are dispersionless, this quantity is given by

$$\Sigma^{<}_{i\phi}=D\int\frac{d\bar{\omega}}{2\pi}G^{<}_{ii}(\bar{\omega})\quad(i=1,2). \tag{23}$$

Equation (23) consists of two equations ($i=1$ and 2), and both $G^{<}_{11}$ and $G^{<}_{22}$ involve $\Sigma^{<}_{1\phi}$ and $\Sigma^{<}_{2\phi}$. The steady-state Green's functions $G^{<}_{ii}(\omega)$ were given in Ref. 18. Equation (23) can be expressed as a system of two linear equations in $\Sigma^{<}_{i\phi}$. In the case of high temperature, where the Fermi functions can be set to $\frac{1}{2}$, it is found from Eq. (23) that $\Sigma^{<}_{i\phi}=iD/2$. For general temperatures, for simplicity we consider the case where the left Fermi level is equal to the right, and the tunnel coupling between the left quantum dot and the left electron reservoir is equal to the right one. Thus Eq. (23) is reduced to

$$-i\Sigma^{<}_{1\phi}=\frac{D}{2}\int\frac{d\bar{\omega}}{2\pi}[f_L(\bar{\omega})\Gamma^L-i\Sigma^{<}_{1\phi}]\times\left[\frac{1}{(\bar{\omega}-\epsilon^0_1+V_{12})^2+\frac{1}{4}(\Gamma^L+\Gamma_{1\phi})^2}+\frac{1}{(\bar{\omega}-\epsilon^0_1-V_{12})^2+\frac{1}{4}(\Gamma^L+\Gamma_{1\phi})^2}\right].$$

Equations (13)–(15) give the current and charge response to the applied ac voltage $V_\alpha(\omega)$ and the internal potential $V_i(\omega)$. When the ac perturbation $eV_\alpha(t)$ and the induced internal potential $\Delta_i(t)$ are transformed to energy coordinates, they must satisfy the relation $\Delta_\alpha(\omega)=[\Delta_\alpha(-\omega)]^*$, $\Delta_i(\omega)=[\Delta_i(-\omega)]^*$. It is easy to see that the positive and negative frequency parts are complex conjugate to each other:

$$G^0_{\alpha\,I}(\omega)=[G^0_{\alpha\,I}(-\omega)]^*\qquad I=1,2,L,R.$$

This is expected, as the ac current is a real-time function. Furthermore, it is easy to show that $G^0_{\alpha I}(\omega)$ and $Q_{i\,I}(\omega)$ fulfill the invariance of current and charge responses under an overall potential shift; that is

$$\sum_{I=1,2,L,R}G^0_{\alpha\,I}(\omega)=0 \tag{24}$$

and

$$\sum_{I=1,2,L,R}Q_{i\,I}(\omega)=0. \tag{25}$$

Büttiker *et al.*[9] indicated that such a time-dependent tunneling response should ensure the overall charge and current conservation. In our above calculation, the piled-up charges on the tunneling junctions and the long-range Coulomb interaction are not included. Next we consider the contribution of capacitive currents and the long-range Coulomb interaction by introducing capacitances between the quantum dots and between the dots and the contacts and the gate electrode; hence we determine the internal potential $\Delta_i(\omega)$ self-consistently. Using a nearest-neighbor capacitance approximation, we have

$$\begin{aligned}Q_1(\omega)&=C_L[V_1(\omega)-V_L(\omega)]+C_d[V_1(\omega)-V_2(\omega)]\\&\quad+C_G[V_1(\omega)-V_G(\omega)],\\Q_2(\omega)&=C_R[V_2(\omega)-V_R(\omega)]+C_d[V_2(\omega)-V_1(\omega)]\\&\quad+C_G[V_2(\omega)-V_G(\omega)],\end{aligned} \tag{26}$$

where C_L (C_R) is the capacitance between the left (right) dot and the left (right) leads, C_g is the capacitance between the dots and a common gate electrode, and C_d is the capacitance between the two dots. Combining Eqs. (26), (13), and (14), we obtain the total current response

$$\begin{aligned}\delta J_{L(R)}(\omega)&=\delta J^{Tun}_{L(R)}(\omega)-i\omega C_{L(R)}[V_{L(R)}(\omega)-V_{1(2)}(\omega)]\\&=\sum_\alpha G_{L(R),\alpha}(\omega)[V_\alpha(\omega)-V_G(\omega)],\end{aligned} \tag{27}$$

therefore, we obtain the frequency-dependent admittance

$$\begin{aligned}G_{L\alpha}(\omega)&=G^0_{LL}(\omega)\,\delta_{L\alpha}-\frac{e^2}{\hbar}\Gamma^L N_{1\alpha}(\omega)-i\frac{e^2}{\hbar}\omega c_L\\&\quad\times\left[\delta_{\alpha L}-\sum_j(M^{-1})_{1j}(\omega)[\Gamma^L N_{j\alpha}(\omega)-C_{j\alpha}]\right]\\&\quad+\sum_{ij}\left(G^0_{Li}(\omega)-\frac{e^2}{\hbar}\Gamma^L N_{1i}(\omega)\right)(M^{-1})_{ij}(\omega)\\&\quad\times[\Gamma^L N_{j\alpha}(\omega)-C_{j\alpha}],\end{aligned} \tag{28}$$

where $M(\omega)$ is the matrix

$$M_{ij}(\omega)=C_{ij}-\Gamma^L N_{ij}(\omega), \tag{29}$$

with

$$C_{11}=(c_L+c_d+c_G),\ C_{12}=-c_d, \tag{30}$$

$$C_{21}=-c_d,\ \ C_{22}=(c_R+c_d+c_G), \tag{31}$$

and

$$C_{i\alpha}=-c_L\delta_{i1}\delta_{L\alpha}-c_R\delta_{i2}\delta_{R\alpha}. \tag{32}$$

Here $c_I=C_I/(e^2/\Gamma^L)$ ($I=L,\ R,\ d$, and G) is capacitance in unit of e^2/Γ^L. $G_{R\alpha}(\omega)$ can be written similarly. Our result fulfills the overall current conservation, that is, $\delta J_L(\omega)+\delta J_R(\omega)+\delta J_G(\omega)=0$.

III. NUMERICAL RESULTS

In this section we present some numerical results for the ac conductance at equilibrium ($\mu_L=\mu_R$) based on Eqs. (13)-(23) and (28). In the wide-band limit, the tunnel couplings

Γ^{α} ($\alpha \in L,R$) are energy-independent constants, and we assume that $\Gamma^{L}=\Gamma^{R}=\Gamma$ for the double quantum dot in our numerical calculations. We also assume that the energy levels of the two dots are equal, i.e., $\epsilon_1^0=\epsilon_2^0=\epsilon_0$.

First we consider the perfect screening case ($c_L=c_R=c_d=c_G=0$).[10] In Fig. 1 we plot the low-temperature ($k_BT=0.01$) ac conductance of a double dot without phonon-electron interaction against the frequency ω for various interdot tunnel couplings V_{12}. The energy levels of the two dots ϵ_0 are set to 0 (all energies are measured in units of Γ), while the identical left and right Fermi levels ($\mu_L=\mu_R=\mu$) are taken to be 2. In Fig. 1(a) we present the real part of the diagonal admittance $\mathrm{Re}[G_{LL}(\omega)]$ as a function of ω for $V_{12}=1$, 2, and 3. The ac conductance at $\omega=0$ should be equal to the dc conductance. We see that for $V_{12}=1$ and 3 $\mathrm{Re}[G_{LL}(\omega)]$ increases as ω increases. It displays a peak at $\omega\sim 2$ for $V_{12}=1$, and two peaks with a distance of about 4 for $V_{12}=3$, but for $V_{12}=2$ it decreases monotonically. This is not surprising, because the so-called photon-assisted tunneling tends the conductance toward a resonant value when the Fermi level deviates from the resonant energy ($\epsilon_0 \pm V_{12}$); however for $V_{12}=2$ the Fermi level is right at the resonant energy. According to the Fermi golden rule, the two peaks of $\mathrm{Re}[G_{LL}(\omega)]$ should appear at the frequency $\omega=|V_{12}\pm\mu|$ (here $\epsilon_0=0$). However, as we pointed out in Ref. 16, the Fermi golden rule alone cannot explain the current behavior here, because the time-dependent voltages make the effective density of states dependent on the frequency. In other words, in Eq. (12) the terms including $\delta\Sigma_{\alpha}^{<}$ can be explained by the Fermi golden rule, but the other terms cannot; this reflects the change of the effective density of states in dots. Thus the position of peaks would deviate from $|V_{12}\pm\mu|$, and delay to a somewhat higher frequency. For $V_{12}=1$ only one peak appears, and for $V_{12}=2$ the second peak also cannot be observed and becomes a ''shoulder'' structure around $\omega\sim 4$. In general when $\mu \geqslant V_{12}$ the second peak is difficult to observe. In this case the Fermi level is outside the two peaks of the density of states (DOS) in the dots. Then the frequency needs to cross over one of the DOS peaks to approach the position of the second peak; thus the height of the second peak is much smaller than that of the first peak. This phenomenon can be seen from Fig. 1(c). We also present the imaginary parts of the diagonal admittance $\mathrm{Im}[G_{LL}(\omega)]$. As expected, all curves show $\mathrm{Im}[G_{LL}(0)]=0$, except that the curve of $V_{12}=2$, $\mathrm{Im}[G_{LL}(\omega)]$, goes to a negative value from zero when the frequency increases from zero; this shows a resistive-capacitive behavior. For the case of Fermi levels at the resonant energy ($V_{12}=2$), $\mathrm{Im}[G_{LL}(0)]$ is always positive; this shows a kinetic-inductive behavior. However, our calculation shows that for a sufficiently large gate capacitance (C_G) and/or lead contact capacitance ($C_{L/R}$), $\mathrm{Im}[G_{LL}(\omega)]$ can be negative for small frequencies even if $\mu=\pm V_{12}$. This is in agreement with the results of Ref. 10 for a single quantum dot system. Similar to $\mathrm{Re}[G_{LL}(\omega)]$, for $\mathrm{Im}[G_{LL}(\omega)]$ there are also two resonant frequencies, which is slightly less than $|V_{12}\pm\mu|$; in contrast, the curves of $\mathrm{Im}[G_{LL}(0)]$ show valleys at the resonant frequency.

In Fig. 2, we plot the admittance G_{LL} against ω for a double quantum dot with electron-phonon interaction ($\Gamma_{\phi}=1$ and 2) and also in the perfect screening case, where $V_{12}=5$ and $\mu=2$. In comparison with the case of free electron-phonon interaction, in Fig. 2 we also plot the curves for $\Gamma_{\phi}=0$. In Fig. 2(a) we present the results for low temperature ($T=0.01$). From this figure, we find that for a double quantum dot with electron-phonon interaction both real and imaginary parts of $G_{LL}(\omega)$ display behaviors similar to that in the case of $\Gamma_{\phi}=0$. However, their resonant amplitudes are seriously suppressed by the phase-breaking effect of electron-phonon interaction, while for small frequencies the nonresonant conductance $\mathrm{Re}G_{LL}(\omega)$ increase as Γ_{ϕ} increases. Qualitatively, this phenomenon is in agreement with the results of Ref. 7, and our result is more prominent than theirs. We believe that this is because we have taken the internal potential of the dots into account. It seems that the suppression to the second resonant peak is more serious, and for $\Gamma_{\phi}=2$ both the second peak of $\mathrm{Re}G_{LL}(\omega)$ and the second valley of $\mathrm{Im}G_{LL}(\omega)$ almost disappear. On the other hand, it is noted that the phase-breaking effect causes the effective capacitance $c_{eff}\sim -d[\mathrm{Im}G_{LL}(0)]/d\omega$ to be reduced; when $\Gamma_{\phi}=2$, the capacitive behavior of the admittance almost changes completely to inductive.

In Fig. 2(b) we present the results for the case of high temperature ($T=50\gg\Gamma$). One can see that, no matter whether we include electron-phonon interaction, the peak structure disappears, and with increasing frequency $\mathrm{Re}G_{LL}(\omega)$ decreases and $\mathrm{Im}G_{LL}(\omega)$ increases monotonically. Furthermore, $\mathrm{Im}G_{LL}(\omega)$ is positive for all frequencies. So for high temperature the admittance always shows an inductive behavior for the perfect screening case. Although the frequency dependence of the admittance is qualitatively similar for $\Gamma_{\phi}=0$ and $\Gamma_{\phi}\neq 0$, the influence of the phase-breaking effect on the admittance is still significant. This point is different from the results of Ref. 7.

Next we investigate the capacitance effect on the admittance of a double quantum dot for low temperature. In Fig. 3, we present the results for the different capacitances considered. Figure 3(a) shows that none of the capacitances has an effect on the real part of the admittance for small frequencies; this is expected. For intermediate frequencies the gate capacitance has the largest effect compared to other capacitances, and the effect of the capacitances between the leads and dots is also quite large. However, the interdot capacitance has almost no effect for small frequencies. For higher frequencies it has a small effect. It is interesting to note that the effects of different capacitances on the value of $\mathrm{Re}G_{LL}(\omega)$ cancel each other partially for intermediate frequencies, but give rise to an additional peak at higher frequencies. Our calculation shows that for sufficiently high frequencies, such an additional peak will appear in all curves in Fig. 3(a) except for the one without capacitance.

In Fig. 3(b), we show the effect of the capacitance on the imaginary part of the admittance. We see that with the capacitances c_G and c_L and c_R, added, respectively, the low-frequency part of the curves of $\mathrm{Im}G_{LL}(\omega)$, move downward, keeping $\mathrm{Im}G_{LL}(0)=0$. Similar to $\mathrm{Re}G_{LL}(\omega)$, there is no effect of c_d on $\mathrm{Im}G_{LL}(\omega)$ for low frequencies. Furthermore,

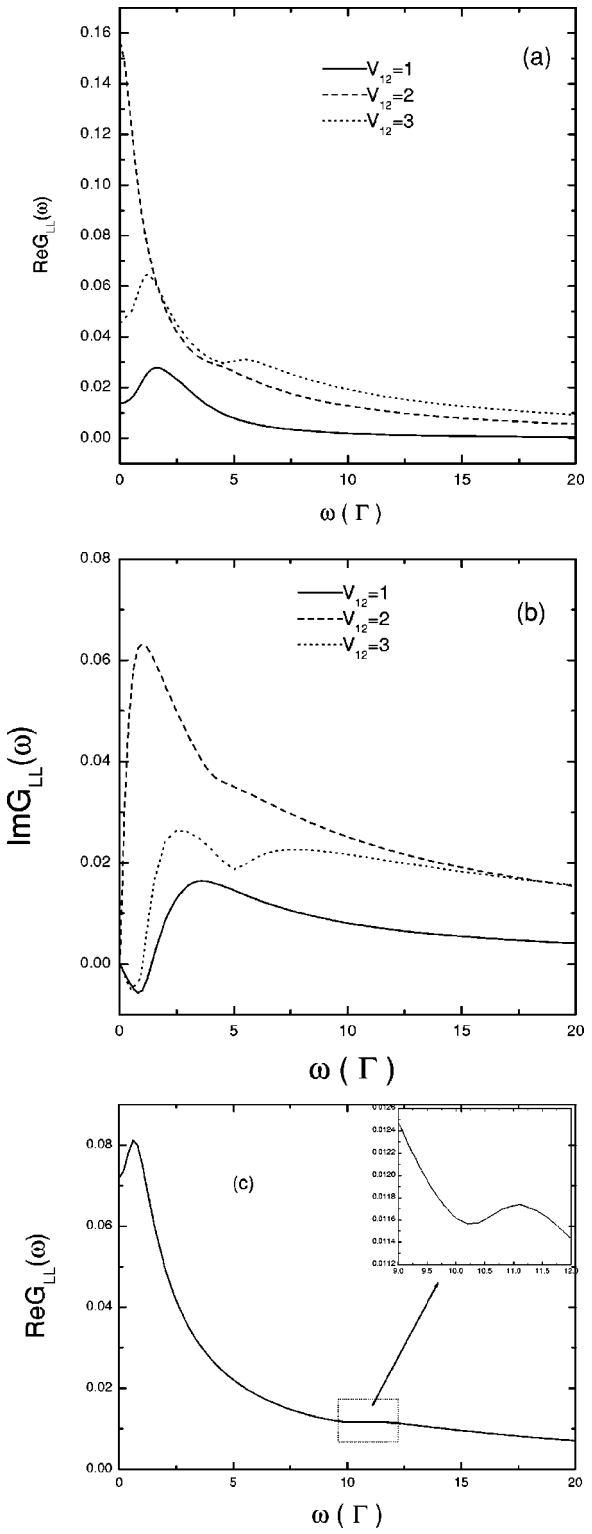

FIG. 1. Plot of the real (a) and imaginary (b) parts of the admittance for a double dot against the frequency. $\epsilon_0=0$, $\mu_L=\mu_R=\mu=2$, $\Gamma_\phi=0$, $kT=0.01$, and $V_{12}=1$ (solid line), 2 (dashed line), 3 (dotted line), and 5 (dot-dashed line). The admittance is measured in units of $e^2/\hbar$, and all energies in units of $\Gamma=\Gamma^L=\Gamma^R$. (b) Real part of the admittance for $\mu=5.5$ and $V_{12}=5$; the other parameters are the same as in (a) and (b). Here all capacitances are taken to be zero.

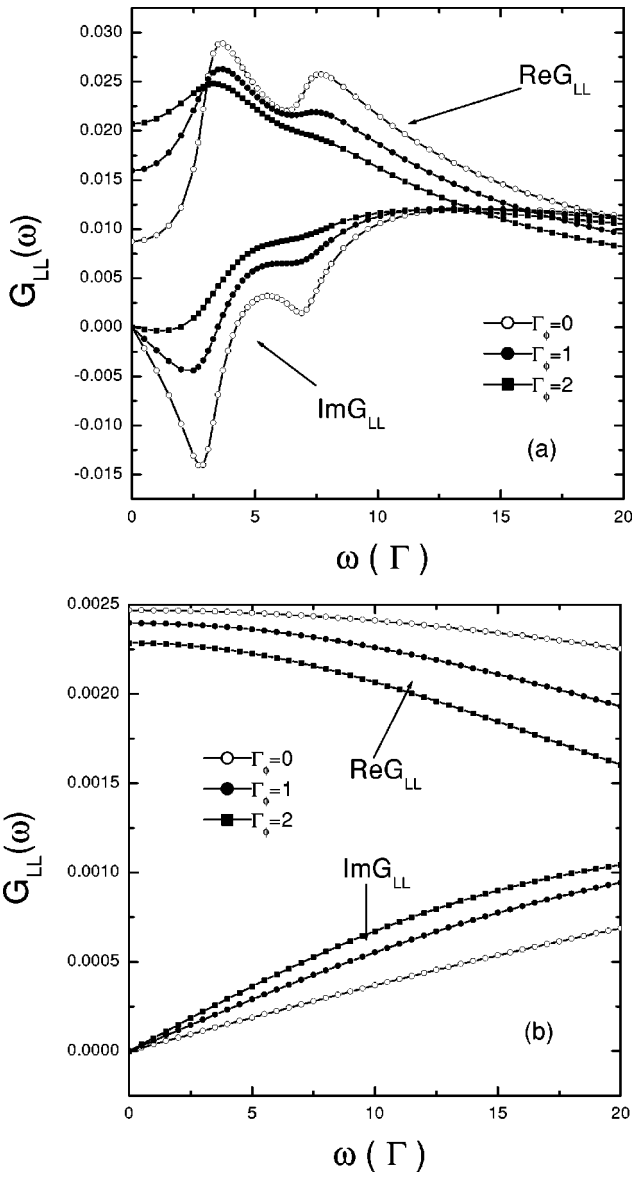

FIG. 2. Plot of the admittance against the frequency of a double dot with and without electron-phonon interaction for low temperature [$T=0.01$ (a)] and high temperature [$T=50$ (b)]. $\epsilon_0=0$, $\mu_L=\mu_R=\mu=2$, and $V_{12}=5$; and $\Gamma_\phi=0$ (open circles), 1 (solid circles), and 3 (solid squares). The admittance is in units of $e^2/\hbar$, and all energies are in units of $\Gamma=\Gamma^L=\Gamma^R$. Here all capacitances are taken to be zero.

when the capacitances are added one by one, we find that for low frequencies Im$G_{LL}(\omega)$ moves down monotonically. In addition, if we use capacitance values different from 0.01, our calculation shows that with an increasing value of the capacitance the curve of Im$G_{LL}(\omega)$ move down monotonically for low frequencies. Therefore, we conclude that by adding capacitances c_G and c_L and c_R into the system, or increasing the values of the capacitances, the effective capacitance $c_{eff}\sim -d\mathrm{Im}G_{LL}(0)/d\omega$ increases, but the interdot capacitance c_d has almost no effect on low-frequency admittance. In Fig. 3(c) we compare the admittances between cases with and without electron-phonon interaction, in the

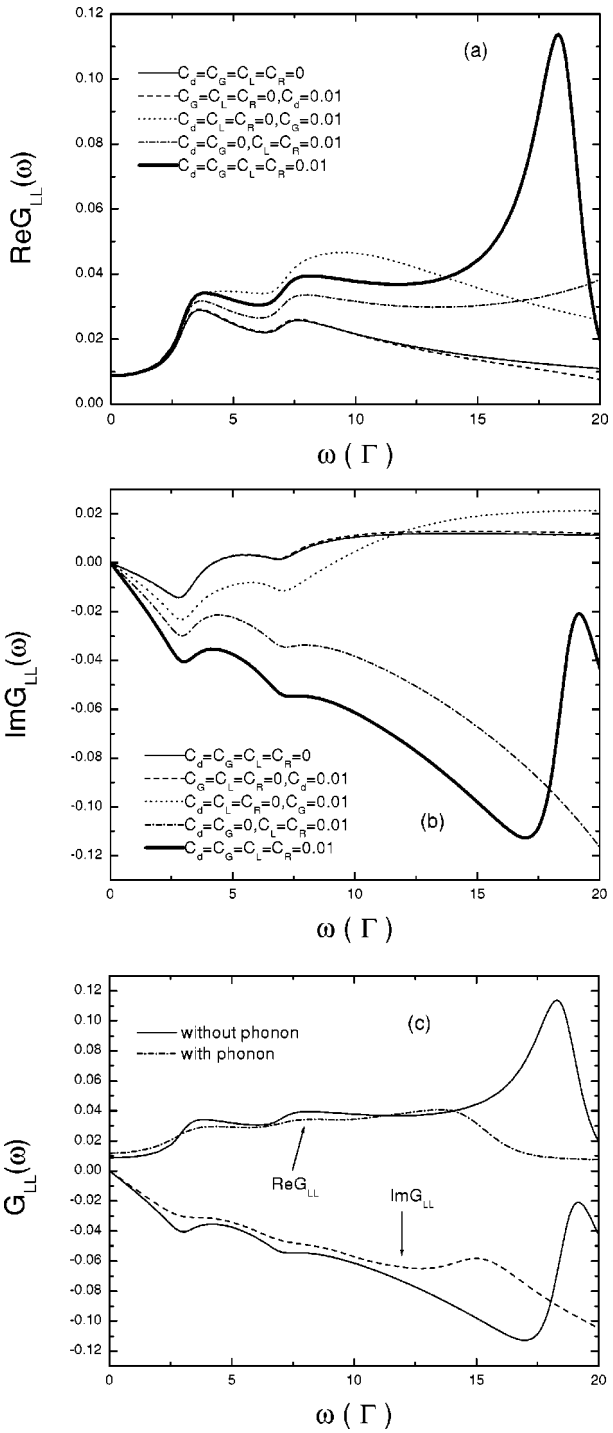

FIG. 3. Plot of the real (a) and imaginary (b) parts of the admittance against the frequency in the presence of capacitances for $c_d = c_L = c_R = c_G = 0$ (solid line), $c_d = 0.01$, and $c_L = c_R = c_G = 0$ (dashed line), $c_G = 0.01$ and $c_L = c_R = c_d = 0$ (dotted line), $c_L = c_R = 0.01$ and $c_d = c_G = 0$ (dot-dashed line), and $c_d = c_L = c_R = c_G = 0.01$ (double solid line). The other parameters are $\epsilon_0 = 0$, $\mu_L = \mu_R = \mu = 2$, $\Gamma_\phi = 0$, $T = 0.01$, and $V_{12} = 5$. The admittance is in units of $e^2/\hbar$, all energies in units of Γ, and capacitances in units of e^2/Γ. (c) A comparison of admittances between cases with and without electron-phonon interaction.

presence of capacitance. One finds that the effect of the electron-phonon interaction is similar to the case without capacitances.

IV. CONCLUSIONS

By calculating nonequilibrium Green's functions, we derived a formula for the linear ac response for a double-dot system with electron-phonon interaction, in the presence of a small ac bias. We have taken into account the capacitances between the leads and dots, between gate electrodes and dots, and dots and dots, and included the displacement currents. The internal time-dependent potentials in the dots are included, and it is determined self-consistently. We therefore reach an overall charge and current conservation. Our results spontaneously fulfill the invariance of current and charge responses under an overall potential shift. We have computed the ac conductance for both $\Gamma_\phi \neq 0$ (with electron-phonon interaction) and $\Gamma_\phi = 0$ (without electron-phonon interaction). The double resonant structure of the ac conductance is observed at low temperature in our results. We find that the resonant peak for $\Gamma_\phi \neq 0$ is much smaller than that for $\Gamma_\phi = 0$, which means that the peak is suppressed by electron-phonon scattering. At high temperature the electron-phonon interaction is also found to have an obvious effect on the ac conductance. Furthermore, we have studied the effect of the capacitance on the ac conductance, and found that for small frequencies the capacitances have less effect on the real part of the admittance; however, except for the dot-dot capacitance they have an obvious effect on the imaginary part. By adding the gate-dot capacitance c_G and the lead-dot capacitances c_L and c_R into the system, and in creasing their values, we find that the effective capacitance $c_{eff} = -d\mathrm{Im}G_{LL}(0)/d\omega$ will increase; however the dot-dot capacitance c_d has almost no effect on low frequency admittance. For high frequencies all the capacitances have considerable effects on the ac conductance.

APPENDIX: EQUATIONS FOR $N_{IJ}(\omega)$ AND $N_{i\alpha}(\omega)$

Using the equation $Q_i(\omega) = -ie\int (d\bar{\omega}/2\pi)\,\delta G^<_{ii}(\bar{\omega} - \omega, \bar{\omega})$, we can obtain the following two coupled equations for the ac charges $Q_i(\omega)$:

$$Q_i(\omega) = \sum_{J=1,2,L,R} e^2[F_{iJ}(\omega) + F^*_{iJ}(-\omega)]V_J(\omega) + \sum_{j=1,2} \Phi_{ij}(\omega)Q_j(\omega), \tag{A1}$$

where

$$F_{11}(\omega) = \int \frac{d\omega_1}{2\pi} G^r_{11}(\omega_1+\omega_0)G^r_{11}(\omega_1)[f_L(\omega_1)\Gamma^L - i\Sigma^<_{1\phi}]G^a_{11}(\omega_1) + V^2_{12}\int \frac{d\omega_1}{2\pi} G^r_{11}(\omega_1 + \omega_0)G^r_{11}(\omega_1)G^{r0}_{22}(\omega_1)[if_R(\omega_1)\Gamma^R + \Sigma^<_{2\phi}]G^{a0}_{22}(\omega_1)G^a_{11}(\omega_1),$$

$$F_{12}(\omega) = +V_{12}^2 \int \frac{d\omega_1}{2\pi} G_{11}^r(\omega_1+\omega_0) G_{11}^{r0}(\omega_1+\omega_0) G_{11}^{r0}(\omega_1)$$
$$\times [f_L(\omega_1)\Gamma^L - i\Sigma_{1\phi}^<] |G_{11}^r(\omega_1)|^2$$
$$+ V_{12}^2 \int \frac{d\omega_1}{2\pi} G_{11}^r(\omega_1+\omega_0) G_{11}^{r0}(\omega_1+\omega_0) G_{11}^{r0}(\omega_1)$$
$$\times [if_R(\omega_1)\Gamma^R + \Sigma_{2\phi}^<] G_{22}^{a0}(\omega_1) G_{11}^a(\omega_1)$$
$$+ V_{12}^4 \int \frac{d\omega_1}{2\pi} G_{11}^r(\omega_1+\omega_0) G_{11}^{r0}(\omega_1$$
$$+ \omega_0) G_{11}^{r0}(\omega_1) G_{22}^{r0}(\omega_1) [f_R(\omega_1)\Gamma^R$$
$$- i\Sigma_{2\phi}^<] G_{22}^{a0}(\omega_1) |G_{11}^a(\omega_1)|^2,$$

$$F_{1L}(\omega) = \Gamma^L \int \frac{d\omega_1}{\pi} \frac{f_L(\omega_1+\omega) - f_L(\omega_1)}{\omega}$$
$$\times G_{11}^r(\omega_1+\omega) G_{11}^a(\omega_1),$$

$$F_{1R}(\omega) = \Gamma^L \int \frac{d\omega_1}{\pi} \frac{f_L(\omega_1+\omega) - f_L(\omega_1)}{\omega}$$
$$\times G_{11}^r(\omega_1+\omega) G_{22}^{r0}(\omega_1+\omega) G_{22}^{a0}(\omega_1) G_{11}^a(\omega_1),$$

and

$$\Phi_{11}(\omega) = D \int \frac{d\omega_1}{2\pi} G_{11}^r(\omega_1+\omega) G_{11}^a(\omega_1),$$

$$\Phi_{12}(\omega) = DV_{12}^2 \int \frac{d\omega_1}{2\pi} G_{11}^r(\omega_1+\omega)$$
$$\times G_{22}^{r0}(\omega_1+\omega) G_{22}^{a0}(\omega_1) G_{11}^a(\omega_1).$$

Analogously, F_{2j}, $F_{2\alpha}$ ($\alpha = L,R$), and Φ_{2j} can be obtained. From Eq. (A1) we therefore obtain Eq. (15), in which $N_{iJ}(\omega)$ reads

$$N_{iJ} = \sum_{j=1,2} [I-\Phi]_{ij}^{-1} [F_{jJ}(\omega) + F_{jJ}^*(-\omega)], \qquad \text{(A2)}$$

where $J = 1, 2, L$, and R, and I is a 2×2 unit matrix.

[1] L.P. Kouwenhoven, S. Jauhar, J. Orenstein, and P.L. McEuen, Phys. Rev. Lett. **73**, 3443 (1994); R.H. Blick, R.J. Hang, D.W. van der Weide, K. von Klitzing, and K. Eherl, Appl. Phys. Lett. **67**, 3924 (1995).

[2] T.H. Oosterkamp, L.P. Kouwenhoven, A.E.A. Koolen, N.C. van der Vaart, and C.J.P.M. Harmans, Phys. Rev. Lett. **78**, 1536 (1997); Nature (London) **395**, 873 (1998).

[3] C. Livermore *et al.*, Science **274**, 1332 (1996).

[4] G. Schedelbeck *et al.*, Science **278**, 1792 (1997).

[5] T.H. Stoof and Yu.V. Nazarov, Phys. Rev. B **53**, 1050 (1996).

[6] A.-P. Jauho, Ned S. Wingreen, and Y. Meir, Phys. Rev. B **50**, 5528 (1994).

[7] M.P. Anatram and S. Datta, Phys. Rev. B **51**, 7632 (1995).

[8] C. Bruder and H. Schoeller, Phys. Rev. Lett. **72**, 1076 (1994); M. Wagner, *ibid.* **76**, 4010 (1996).

[9] M. Büttiker, A. Pretre, and H. Thomas, Phys. Rev. Lett. **70**, 4114 (1993); T. Christen and M. Büttiker, Phys. Rev. B **53**, 2064 (1996).

[10] A. Pretre, H. Thomas, and M. Büttiker, Phys. Rev. B **54**, 8130 (1996).

[11] C.A. Stafford and Ned S. Wingreen, Phys. Rev. Lett. **76**, 1916 (1996).

[12] H.K. Zhao, Phys. Lett. A **226**, 105 (1997).

[13] T. Ivanov, Phys. Rev. B **56**, 12 339 (1997).

[14] Zhongshui Ma, Junren Shi, and X.C. Xie, Phys. Rev. B **62**, 15 352 (2000).

[15] Y.B. Yu, T.C. Au Yeung, W.Z. Shangguan, and C.H. Cham, Phys. Lett. A **275**, 131 (2000).

[16] Yabin Yu, T.C. Au Yeung, W.Z. Shangguan, and C.H. Kam, Phys. Rev. B **63**, 205314 (2001).

[17] L.J. Geerlings, V.F. Anderegg, P.A.M. Holweg, J.E. Mooij, H. Pothier, D. Esteve, C. Urbina, and M.H. Devoret, Phys. Rev. Lett. **64**, 2691 (1990).

[18] W.Z. Shangguan, T.C. Au Yeung, Y.B. Yu, and C.H. Kam, Phys. Rev. B **63**, 235323 (2001).

[19] C. Lacroix, J. Phys. F **11**, 2389 (1981).

[20] H. Haug, and A.-P. Jauho, *Quantum Kinetics in Transport and Optics of Semiconductors* (Springer-Verlag, Berlin, 1996).